CI Cygni 2010 Outburst and Eclipse: An Amateur Spectroscopic Survey—First Results From Low Resolution Spectra

François Teyssier
67 Rue Jacques Daviel, Rouen 76100, France; francois.teyssier@dbmail.com

Received January 10, 2011; revised February 10, 2011; accepted February 11, 2011

Abstract The aim of this document is to present the amateur spectroscopic survey of the 2010 outburst of symbiotic star CI Cygni by Christian Buil, Thierry Garrel, Benjamin Mauclaire, François Teyssier, Eric Sarrazin, and Pierre Dubreuil (ARAS—Astronomical Ring for Access to Spectroscopy). This outburst coincides with an eclipse of the hot component by the late-type giant star. After a brief review of the current knowledge of this system, the campaign is presented. The first results obtained from low-resolution spectra are described: main emission lines (equivalent width and absolute flux) and continuum evolution in comparison with the CCD *V* light curve obtained by AAVSO observers.

1. Introduction

Symbiotic stars are binary systems composed of a cool giant and a hot, luminous white dwarf, surrounded by an ionized nebula. CI Cyg is a symbiotic star containing a cool giant of type M5.5II (Mürset and Schmid 1999) and a compact star. CI Cyg is one of the very few symbiotic systems in which the giant fills or nearly fills its Roche lobe and shows ellipsoidal photometric variations in its light curve, especially in *R* and near-IR bands (Mikołajewska 2003).

From UV observations, Kenyon *et al.* (1991) argued that the compact star should be a $0.5M_{\odot}$ main sequence star surrounded by an extended accretion disk. The high temperature of the hot component (T = 125,000 K) allows the formation of high ionization emission lines (HeII, [Fe VII]) observed in CI Cyg during quiescence. The nature of the hot component is still controversial. On the one hand, Mikołajewska and Kenyon (1992) considered that the evolution during the outburst is best explained by the presence of an unstable thick disk around the main sequence accretor. On the other hand, Mikołajewska (2003) estimates that the quiescent characteristics of the hot component are more consistent with a hot and luminous white dwarf powered by nuclear burning of the accreted hydrogen. During outbursts the temperature is much lower ($T \leq$ 20,000 K). The higher excitation lines thus vanish as the outburst progress. This could be explained by a large expansion in the radius of the accreting star. The expansion of the pseudo-photosphere causes it to cool. The energy peak of the pseudo-photosphere shifts from the far UV to optical range, causing the star to appear in "outburst" (Siviero *et al.* 2009).

At quiescence, the spectrum is dominated by the molecular absorption bands of the cool giant star, Balmer, HeI, and high ionization emission lines (HeII, [Fe VII]) powered by the very hot companion (Figure 1).

Eclipses have been detected in the light curve. The permitted emission lines show a pronounced eclipse effect. The lack of eclipse in forbidden emission lines suggests that they are emitted in a much larger region than the Balmer and Helium lines (Mikołajewka 1985).

As shown in Figure 2, the M giant fills its Roche lobe and transfers material into an extended disk surrounding the hot component. The disk is surrounded by a small He II region and a larger HeI, [OIII] zone. A larger highly ionized region ([FeVII], [NeIII]) has been detected in eclipse studies, but its geometry remains uncertain.

This system shows classical symbiotic outbursts. Those of 1911 and 1937 were minor ones in brightness amplitude and duration. Between 1970 and 1978, CI Cyg underwent an active phase consisting of several optical brightenings with amplitudes up to 2 magnitudes, with 3 maxima occurring in November 1971, November 1973, and August 1975. A sharp minimum, centered on October 4, 1975, was caused by a total eclipse of the outbursting component by the giant star (Figure 3). After a long quiescent state, lasting for three decades, a new series of outbursts began in 2008 (AAVSO 2008).

The 2010 outburst was first detected by Munari *et al.* (2010). This outburst coincides with an eclipse of the hot component.

2. Observations

High and low resolution spectra were acquired by several amateurs in France (Table 1). The fit and dat files can be downloaded from:

http://www.astrosurf.com/aras/CICyg/CI_Cyg.html

68 spectra low and high resolution spectra were acquired between June 30 and December 25, 2010.

A few spectra were acquired using a slitless 100l/mm spectrograph (StarAnalyser) by Eric Sarrazin and Pierre Dubreuil. eShel, Lhires, and Lisa are Shelyak Instruments products. Some samples of spectra at different resolutions are shown in Figures 4a through 4d.

3. Luminosity curve from AAVSO data

The photometric evolution of CI Cygni is presented in Figure 5. Up to July 20, 5-day mean visual data are used (dotted line). The solid line shows the daily-mean CCD-*V* data since July 20. The luminosity increased irregularly for about three months from Vis = 11.2 to a maximum $V = 9.8$ (August 26) with a mean increase of –0.013 mag d^{-1}. This rate shows significant accelerations especially

between July 22 and 31 and between August 16 and 26 with, respectively, –0.032 and – 0.036 mag d^{-1} rates. This almost stage-by-stage rise looks like the Z And outburst in 2000 (Bisikalo *et al.* 2006) though the plateaus are less marked.

The eclipse began on August 26 (JD 2455435) and ended on November 14 (JD 2455515) with a total duration of 80 days. This is much shorter than the 1975 eclipse duration established at 130 days (Mikołajewska and Mikołajewski 1983). The eclipse ingress is quite linear with minor variations in the slope, with a mean value of 0.035 mag d^{-1}. During the totality, the profile shows a U shape (from September 29 to October 26—JD 2455469 to 2455496) and went through the minimum on October 14 (JD 2455484) at $V = 11.16$. The totality duration was 30 days, also much less than during 1975 (72 days estimated by Mikołajewska and Mikołajewski 1983).

The eclipse egress lasted 16 days, with a mean rate of 0.019 mag d^{-1}, and ended at $V \sim 10.7$. The luminosity has been almost stable since the eclipse ended.

The comparison of profiles (Figures 6a and 6b) shows that the 2010 outburst was much shorter than 2008-2009 and 1975 ones.

The 1975 and 2010 eclipse profiles (Figure 7) have been plotted according to phase computed with the following ephemeris: Min(V) = 2 442 690 + 853.8E, where the epoch is the photocenter of the 1975 eclipse and the period is adopted from Fekel *et al.* (2000).

The minimum luminosity occurs at phase = –0.02, i.e., 18 days before the minimum predicted by the spectroscopic ephemeris. The profile is narrower than for the 1975 eclipse and less symmetric.

4. Spectral evolution

The spectral evolution was studied using low resolution spectra obtained with a 25-cm Schmidt Cassegrain telescope (F/D 10), a Starlight SXV-H9 CCD, and a Lhires III spectrograph with a 150 l/mm grating. The dispersion is 2.14 Å/pixel and the resolution about 800.

The spectra were reduced with standard procedures, including the use of a standard star observation to correct for the wavelength-dependent spectral response.

The spectral evolution is described in Figures 8 and 9.

The outburst progressed from June 30 to August 23. The spectral variation shows the dramatic disappearance of the high excitation lines, especially [FeVII]. The molecular absorption bands strongly weaken; they are partially filled by the emission from the hot components (Figure 8a).

From August 24 (when the eclipse begins while the outburst is still in progress), to October 14 (at mid-eclipse), the continuum changes in the reverse way: the absorption bands strengthen (Figure 8b). At mid-eclipse, the continuum is quite the same as at the beginning of the outburst. The high ionization [Fe VII] reappeared slightly, which shows the rise in temperature and the decline of outburst.

The complete evolution is described in Figure 9, in which spectra are in absolute flux.

5. Equivalent width variations

Equivalent widths have been measured on Hα, Hβ, HeI, HeII, and [OIII] lines. The Hα EW was measured directly. For the other lines, a Gaussian fit was used. This allowed the lines to be deblended, notably the [OIII]/HeI lines.

The Ha equivalent width monotonically increased from June 30 to August 18, followed by a sudden decrease of 13% which coincided with a luminosity burst. The monotonic increase then returned up to October 20.

At that time, a new sudden decrease of 14% was detected, eight days after eclipse maximum. From October 20 EW Hα increased again monotonically. This evolution is plotted in Figures 10a through 10d where squares are low spectra values and crosses are values obtained from eShel spectra by Christian Buil.

The general shape of Hβ and Hα EW are similar, with decreases seen in the EW curves at the same time.

The He II λ 4686 EW curve is completely different. The light curve and EW HeII look remarkably similar. HeII is the only line whose EW evolution is clearly correlated with the photometric curve during the eclipse phase.

The [OIII]/He I ratio (Figure 11) was almost stable up to mid-September (~15th), varying from 1.5 to 1.9. It then increased suddenly to a maximum value of 12.6 on October 16 (JD 245586), at phase –0.009, eight days before the predicted date.

The decrease in ratio is nearly linear, with a greater slope (+40% compared to the rising slope), to a minimum of 2.6, slightly greater than the value before eclipse.

6. Line variations in absolute flux

An absolute flux calibration has been obtained by scaling the continuum by the CCD-*V* magnitude in the range 530–582 nm (O'Connell 1973). The conversion of *V* magnitude to absolute flux has been computed using the Spitzer Science Center Magnitude to Flux Density Converter which overestimates the result by a factor of 1.05 compared with the classical formula: $\log F\lambda = -0.400V - 8.449$ erg × s^{-1} × cm^{-2} × $Å^{-1}$.

The HI, HeI, and HeII absolute flux and luminosity curves look remarkably similar, except that the flux continues to increase after the eclipse ends while the *V* magnitude is almost stable (Figure 12). All these lines show pronounced eclipse effects. The intensity at mid-eclipse is about half the pre-eclipse value for HI lines, 1/6 for HeII λ 4686, and 1/3 for HeI λ 5876. These values are similar to those estimated during the 1975 eclipse (Mikołajewka and Mikołajewski 1983).

The [OIII] λ 5007 flux measurements are more scattered (Figure 13). There is no detectable eclipse effect. The [OIII] emission region is more extended than the HI, HeI, and HeII zone (Mikołajewska and Mikołajewski 1983). The maximum intensity occurred around September 25 (JD 2455465).

7. Continuum variations

At the beginning of the outburst (June 30) the continuum matched correctly with a M5III standard star, HD 221615, from The Indo-U.S. Library of Coudé Feed Stellar Spectra (Figure 14a).

As the outburst progressed the absorption bands reduced. At maximum luminosity, the continuum does not match any earlier spectral type continuum (M3 or M4). A synthetic spectrum has been computed consisting of a M5III spectrum and a HI recombination continuum at T = 5,000 K (Osterbrock and Ferland 2006). This is an approximate value which is nevertheless consistent with the value of 7,600K for the nebular emission derived by Skopal (2003) when CI Cyg is in outburst. The result is shown in Fig 14b.

The continuum variations have been measured using two TiO indices as defined by Kenyon and Fernandez Castro (1987). TiO1 measures the 6125 Å TiO band while TiO2 measures the 7025 Å TiO band. As illustrated in Figure 15, the two TiO indices are strongly correlated with luminosity *V* curve.

The high degree of correlation is illustrated by the graphs showing TiO index as a function of *V* magnitude (Figures 16a and 16b).

9. Acknowledgements

I would like to thank the AAVSO visual and CCD observers who acquired the photometric data used in this document and especially for CCD measurements: Teofilo Arranz, Emery Erdelyi, Geir Klingenberg, Kenneth Menzies, Stephen Riley, Jari Suomela, Ray Tomlin, Paolo Corelli, Juan-Luis Gonzalez Carballo, Peter Kalajian, Artyom Novichonok, Marzio Rivera, Richard Sabo, Charles Trefzger, Tim Crawford, Keith Graham, David Lane, Martin Nicholson, Douglas Slauson, Andras Timar, and Jani Virtanen.

I gratefully acknowledge Dr. Michael Friedjung (IAP) for his very helpful advice.

References

AAVSO 2008, *AAVSO Special Notice #121* (August 31).

Bisikalo, D. V., Boyarchuck, A. A., Kilpio, E. Yu., Tomov, N. A., and Tomova, M. T. 2006, *Astron. Rep.*, **50**, 722.

Fekel, F. C., Joyce, R. R., Hinkle, K. H., and Skrutskie, M. F. 2000, *Astron. J.*, **119**, 1375.

Kenyon, S. J., and Fernandez Castro, T. 1987, *Astron. J.*, **93**, 938.
Kenyon, S. J., Oliversen, N. A., Mikołajewska, J., Mikołajewski, M., Stencel, R. E., Garcia, M. R., and Anderson, C. M. 1991, *Astron. J.*, **101**, 637.
Munari, U., Siviero, A., Cherini, G., Dallaporta, S., and Valisa, P. 2010, *Astron. Telegram*, Nr. 2732, 1.
Mikołajewska, J., 1985, *Acta Astron.*, **35**, 65.
Mikołajewska, J. 2003, in *Symbiotic Stars Probing Stellar Evolution*, ASP Conference Proceedings, Vol. 303, R. L. M. Corradi, R. Mikołajewska, and T. J. Mahoney, eds., Astronomical Society of the Pacific, San Francisco, p.9.
Mikołajewska, J., and Kenyon, S. J. 1992, *Mon. Not. Roy. Astron. Soc.*, **256**, 177.
Mikołajewska, J., and Mikołajewski, M. 1983, *Acta Astron.*, **33**, 403.
Mürset, U., and Schmid, H. M. 1999, *Astron. Astrophys. Suppl. Ser.*, **137**, 473.
Osterbrok, D. E., and Ferland, G. F. 2006, *Astrophysics of Gaseous Nebulae and Active Galactic Nuclei*, University Science Books, Mill Valley, California.
Skopal, A. 2003, arXiv:astro-ph/0308462v1.
Siviero, A., *et al.* 2009, *Mon. Not. Roy. Astron. Soc.*, **399**, 2139.

Table 1. Observers of high resolution spectra of CI Cyg.

Observer	*Telescope*	*Spectrograph*	*Resolution*	*Approx. Range*	*Nr. spectra*
C. Buil	SC 28cm	eShel	11 000	428–712 nm	16
T. Garrel	SC 21 cm	LHIRES III 2400 l/mm	15 000	650–661 nm	13
B. Mauclaire	SC 21 cm	LHIRES III 2400 l/mm	15 000	652–669 nm	4

Table 2. Observers of low resolution spectra of CI Cyg.

Observer	*Telescope*	*Spectrograph*	*Resolution*	*Approx. Range*	*Nr. spectra*
C. Buil	SC 23 cm	LISA 300 l/mm	1000	390–730 nm	1
F. Teyssier	SC 25 cm	LHIRES III 150 l/mm	800	440–720 nm	34

Table 3. Emission line equivalent width (Å).

Nr.	*Date*	*JD 2450000*	*Phase*	*Ha*	*Hb*	*HeII 4686Å*	*HeI 5876Å*	*[OIII] /HeI*
1	30/06/2010	5378.417	–0.135	124	44.2	50.2	15.2	2.1
2	24/07/2010	5402.393	–0.107	147	54.0	62.4	26.0	1.7
3	02/08/2010	5411.403	–0.097	156	55.1	65.0	27.4	1.6
4	09/08/2010	5417.534	–0.090	167	57.1	64.3	28.9	1.4
5	18/08/2010	5427.390	–0.078	173	57.2	60.3	29.0	1.8
6	23/08/2010	5432.330	–0.072	149	43.0	45.0	26.1	1.7
7	30/08/2010	5439.333	–0.064	172	45.3	53.5	31.2	2.2
8	01/09/2010	5441.426	–0.062	178	48.7	50.4	29.6	1.7
9	04/09/2010	5444.440	–0.058	184	52.7	48.2	30.4	1.9
10	08/09/2010	5448.330	–0.054	194	56.9	47.8	30.4	1.9
11	10/09/2010	5450.335	–0.051	198	57.0	48.0	28.6	1.9
12	17/09/2010	5457.383	–0.043	206	62.6	43.6	30.6	
13	18/09/2010	5458.325	–0.042	210	65.4	30.8	4.3	
14	21/09/2010	5461.396	–0.038	219	67.5	32.9	3.8	
15	22/09/2010	5462.389	–0.037	228	74.1	43.7	31.8	3.8
16	25/09/2010	5465.360	–0.034	234	84.1	41.8	36.0	
17	30/09/2010	5470.300	–0.028	242	87.2	31.6	34.9	6.8
18	07/10/2010	5477.325	–0.020	248	88.5	24.8	33.6	8.9
19	09/10/2010	5479.317	–0.017	248	90.5	23.2	34.3	
20	10/10/2010	5480.300	–0.016	243				
21	12/10/2010	5482.325	–0.014	251	90.3	22.0	35.8	11.9
22	16/10/2010	5486.316	–0.009	261	90.8	19.5	36.4	12.6
23	17/10/2010	5487.301	–0.008	263	89.6	19.9	30.6	
24	20/10/2010	5490.309	–0.004	272	87.0	23.3	32.9	
25	22/10/2010	5492.278	–0.002	248	87.7	22.2	30.9	10.1
26	25/10/2010	5495.271	0.001	239	90.3	23.1	30.7	10.7
27	30/10/2010	5500.291	0.007	234	87.7	20.0	31.4	7.6
28	31/10/2010	5501.285	0.009	229	85.7	21.5	31.5	7.0
29	01/11/2010	5502.275	0.010	229	82.1	20.9	33.9	
30	07/11/2010	5508.244	0.017	239	85.3	26.1	33.5	5.7
31	20/11/2010	5521.273	0.032	254	86.6	34.1	40.0	3.0
32	03/12/2010	5534.290	0.047	305	91.1	44.4	40.1	
33	12/12/2010	5543.252	0.058	327	91.3	46.3	39.6	2.6
34	14/12/2010	5545.213	0.060	317	94.9	45.4	40.3	2.5
35	25/12/2010	5556.250	0.073	350	105.0	64.5	43.2	2.7

Table 4. Emission line absolute flux (10^{-12} erg × cm^{-2} × s^{-1}).

Nr.	*Date*	*JD 2450000*	*Phase*	*Ha*	*Hb*	*HeI 5876Å*	*HeII 4686Å*	*[OIII] 5007Å*
1	30/06/2010	5378.417	–0.135	48	5.1	2.3	5.2	0.6
2	24/07/2010	5402.393	–0.107	65	7.8	4.6	8.1	1.2
3	02/08/2010	5411.403	–0.097	96	8.0	7.6	8.8	1.9
4	09/08/2010	5417.534	–0.090	100		8.9	10.8	2.4
5	18/08/2010	5427.390	–0.078	110	10.5	8.6	10.4	2.8
6	23/08/2010	5432.330	–0.072	128	9.7	10.1	10.9	3.0
7	30/08/2010	5439.333	–0.064	141	11.5	12.4	13.0	
8	01/09/2010	5441.426	–0.062	133	10.1	11.1	9.7	2.9
9	04/09/2010	5444.440	–0.058	134	9.6	10.3	8.5	2.9
10	08/09/2010	5448.330	–0.054	116	11.4	9.4	10.0	3.3
11	10/09/2010	5450.335	–0.051	129	8.4	9.1	6.8	2.9
13	18/09/2010	5458.325	–0.042	84	10.4	6.6	7.0	3.6
15	22/09/2010	5462.389	–0.037	94	10.1	6.4	6.1	4.0
16	25/09/2010	5465.360	–0.034	88	9.1	6.0	4.0	3.8
17	30/09/2010	5470.300	–0.028	72	8.6	4.2	3.1	3.3
18	07/10/2010	5477.325	–0.020	77	6.4	3.7	1.7	2.9
22	16/10/2010	5486.316	–0.009	71	6.6	4.1	1.3	3.5
24	20/10/2010	5490.309	–0.004	77	7.4	4.2	1.8	3.5
25	22/10/2010	5492.278	–0.002	83	6.3	4.3	1.5	3.0
26	25/10/2010	5495.271	0.001	64	6.2	3.9	1.7	3.0
29	01/11/2010	5502.275	0.010	70	7.2	4.4	2.1	3.4
30	07/11/2010	5508.244	0.017	86	7.9	5.3	2.6	3.0
31	20/11/2010	5521.273	0.032	94	9.5	6.6	3.6	2.5
32	03/12/2010	5534.290	0.047	125		8.0	5.2	3.1
33	12/12/2010	5543.252	0.058	138	10.4	8.4	4.4	2.5
34	14/12/2010	5545.213	0.060	140	11.5	8.4	4.4	2.7
35	25/12/2010	5556.250	0.073	160	13.2	10.6	7.1	3.0

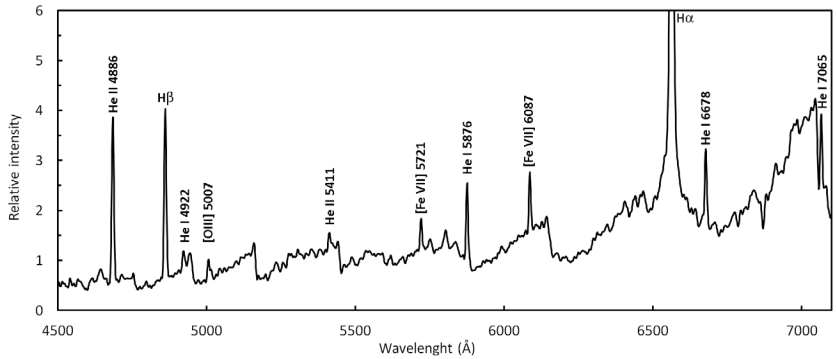

Figure 1. CI Cygni spectrum at the beginning of the outburst (2010 June 30). The Hα line has been truncated in favor of the fainter features.

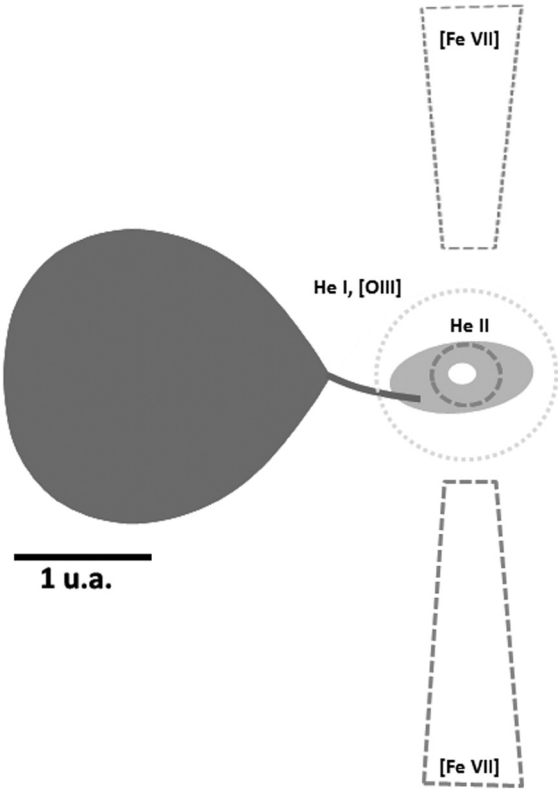

Figure 2. A schematic representation of CI Cyg adapted from Kenyon *et al.* (1991).

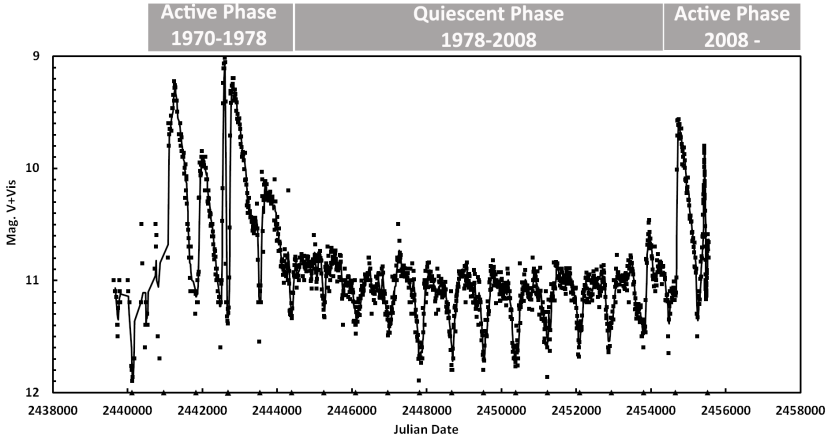

Figure 3. Long term light curve (Visual and CCD-V 10-day mean) from AAVSO observers. Eclipses are marked by triangles.

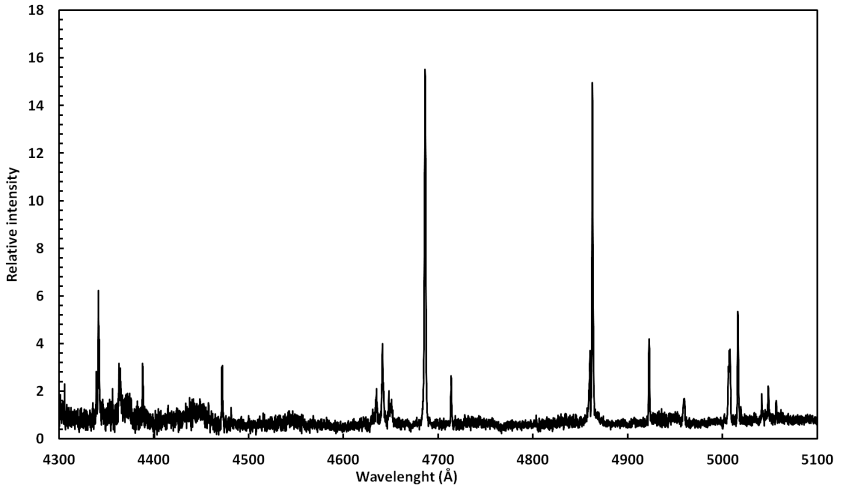

Figure 4a. Part of an eShel spectrum (R = 11000), with line identification by Christian Buil.

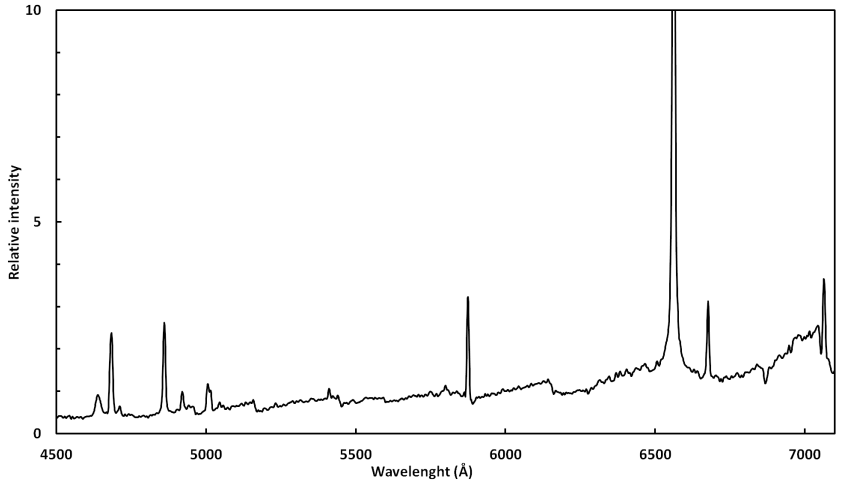

Figure 4b. Low resolution (R = 800) by François Teyssier.

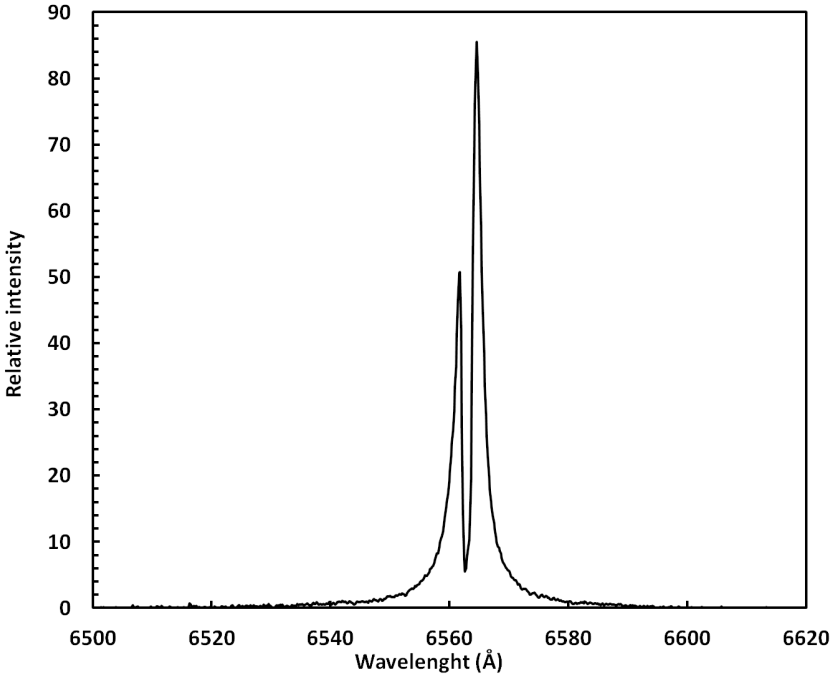

Figure 4c. High resolution spectrum of the Hα line (R = 15000) by Thierry Garrel.

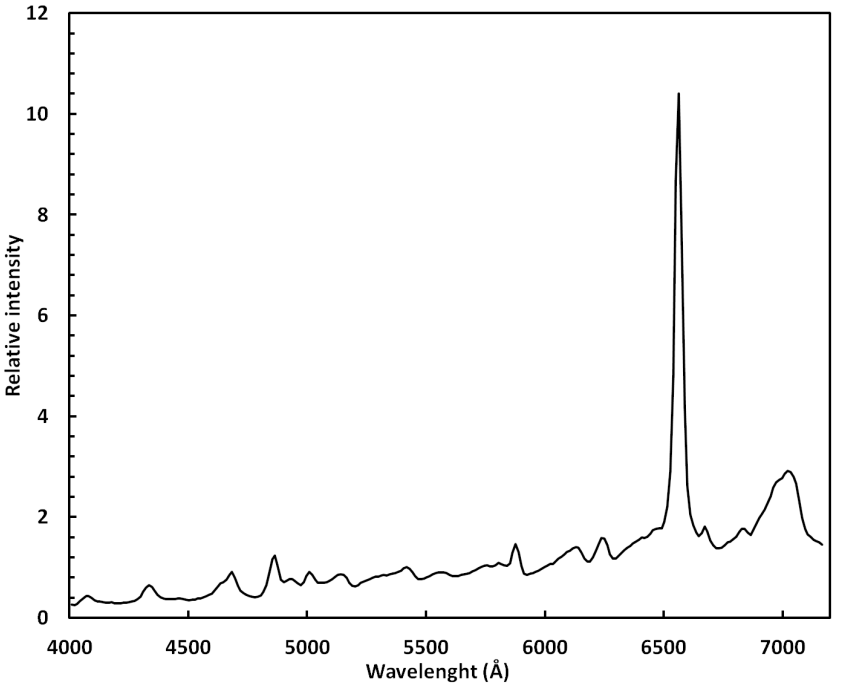

Figure 4d. Very low resolution (slitless Star Analyser) by Eric Sarrazin.

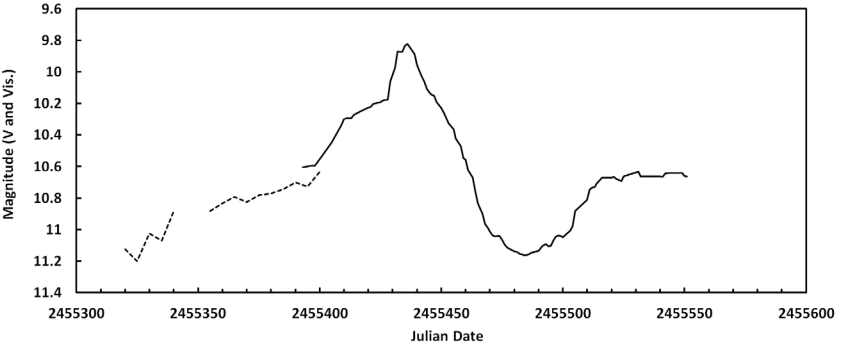

Figure 5. Visual (dotted line) and CCD-V (solid line) light curve from AAVSO data.

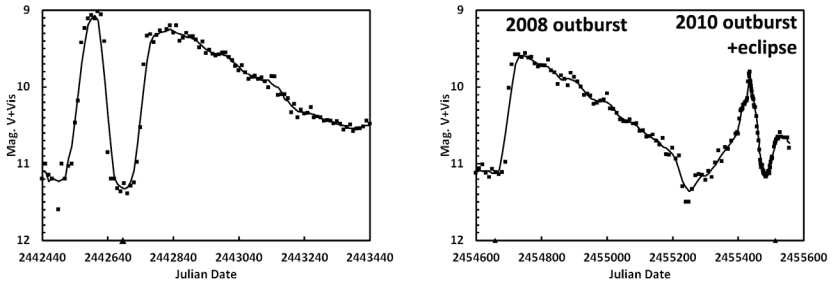

Figure 6. Comparison of 1975 and 2010 outbursts and eclipses photometric profiles. Figure 6a (left): 1975 outburst and eclipse. Figure 6b (right): 2008–2010 outbursts and 2010 eclipse.

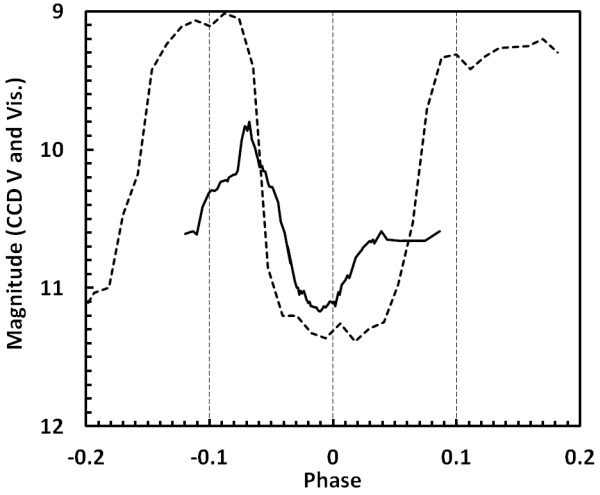

Figure 7. 1975 (dotted line) and 2010 (solid line) eclipse profiles according to phase.

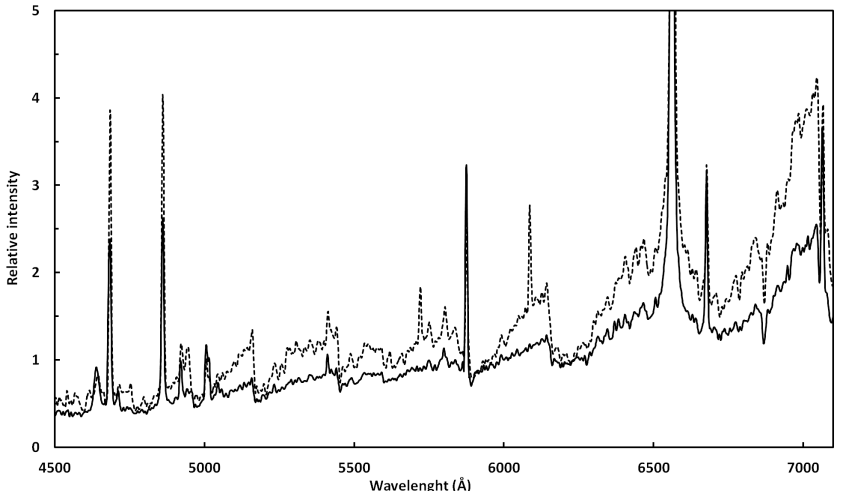

Figure 8a. Spectral evolution of CI Cyg between 2010 June 30 (dotted line) and 2010 August 24 (solid line).

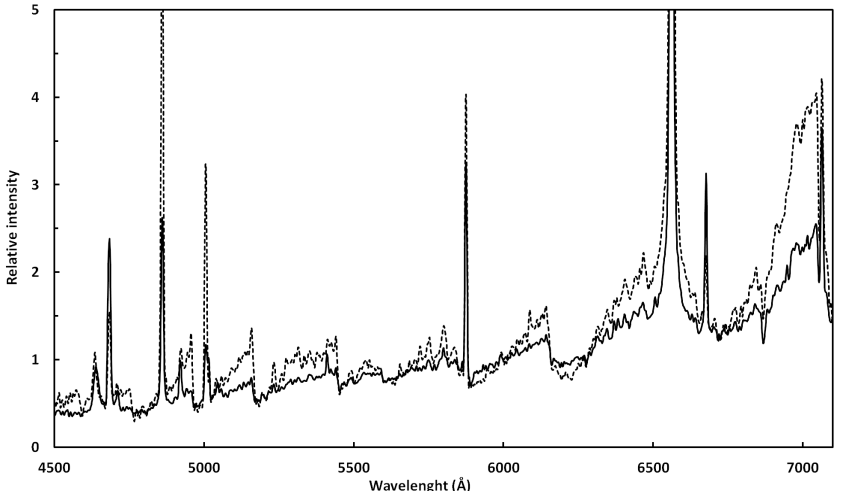

Figure 8b. Spectral evolution between 2010 August 24 (solid line) and 2010 October 14 (dotted line).

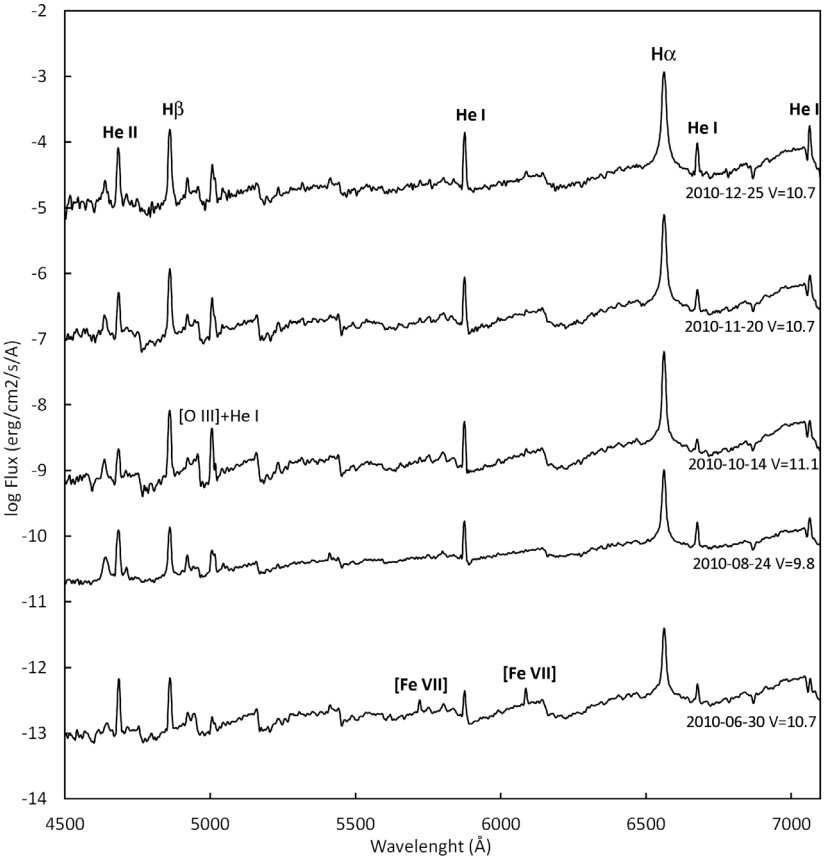

Figure 9. Absolute flux spectral evolution of CI Cyg during the 2010 outburst. For clarity, the spectra are offset in ordinates by 2 units.

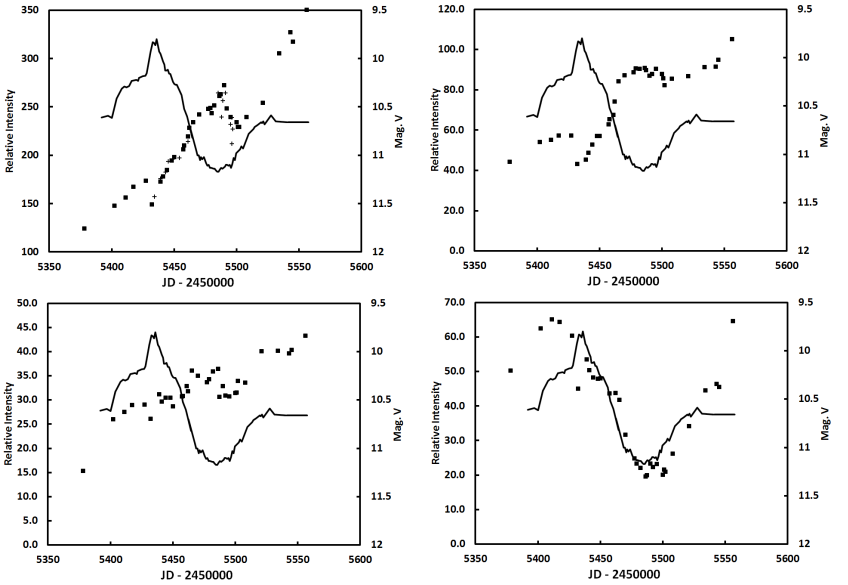

Figure 10. Equivalent widths time series (JD 2450000). Squares for low resolution values, crosses for eShel values (only Hα). Figure 10a (top left): Hα equivalent width. Figure 10b (top right): Hβ equivalent width. Figure 10c (bottom left): HeI λ5876 equivalent width. Figure 10d (bottom right): HeII λ4686 equivalent width.

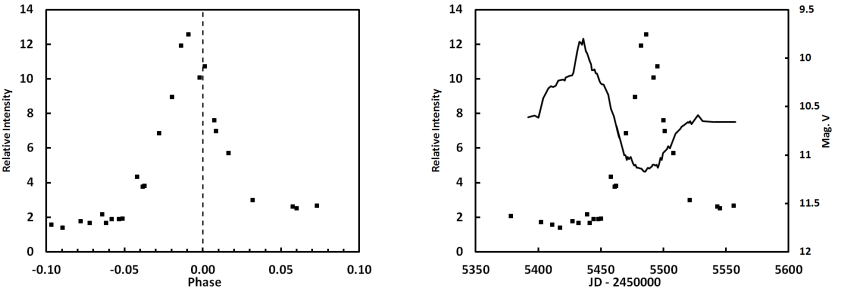

Figure 11a (left). [OIII]/HeI 5016 EW ratio as a function of phase. Figure 11b (right). [OIII]/HeI 5016 EW ratio as a function of JD. CCD-*V* light curve, solid line.

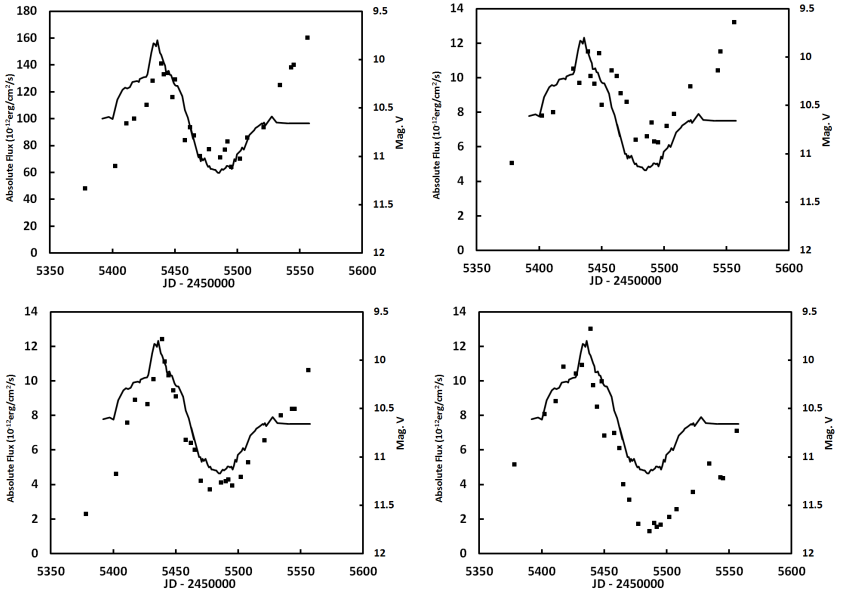

Figure 12. Absolute line flux (erg × $^{s-1}$ × cm^{-2} × Å^{-1}) as a function of time (JD-2450000) and CCD light curve, as solid line). Figure 12a (top left): Hα absolute flux. Figure 12b (top right): Hβ absolute flux. Figure 12c (bottom left): HeI λ 5876 absolute flux. Figure 12d (bottom right): HeII λ4686 absolute flux.

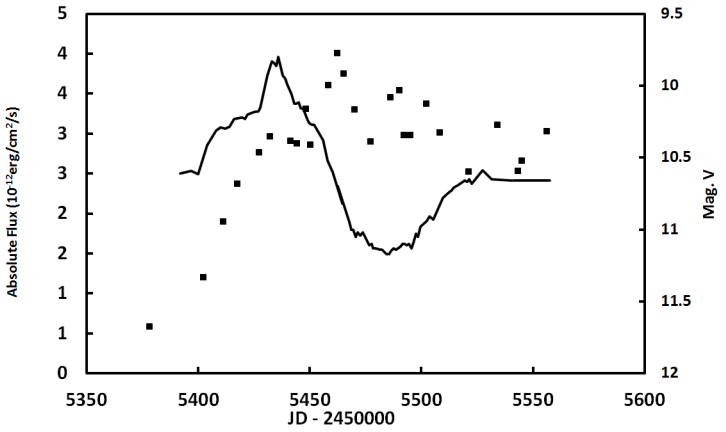

Figure 13. [OIII] l 5007 absolute flux evolution.

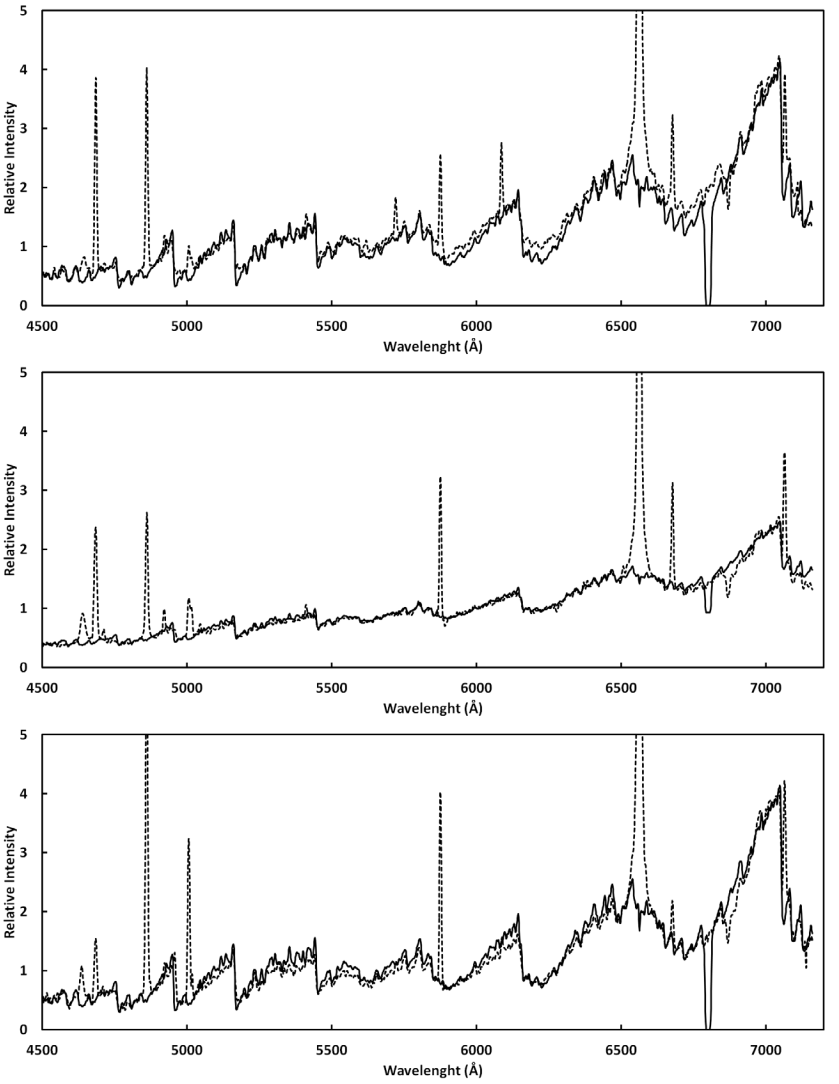

Figure 14. CI Cygni spectra: dotted lines; Comparison spectra: solid lines. Figure 14a (top): Comparison between the 2010 June 30 spectrum (dotted line) and a M5III standard. Figure 14b (middle): At max luminosity (August 24), the continuum matches a synthetic spectrum: M5III composite with a HI recombination continuum (T = 5000 K). Figure 14c (bottom): At mid-eclipse, the continuum again matches a M5 III standard.

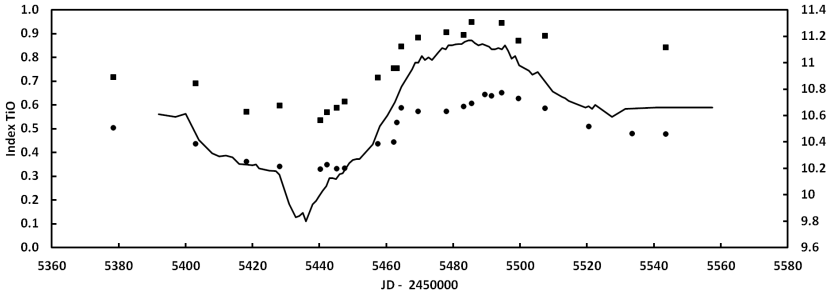

Figure 15. TiO index variation as a function of JD (2450000) and V magnitude (solid line). TiO_1, squares; TiO_2, circles.

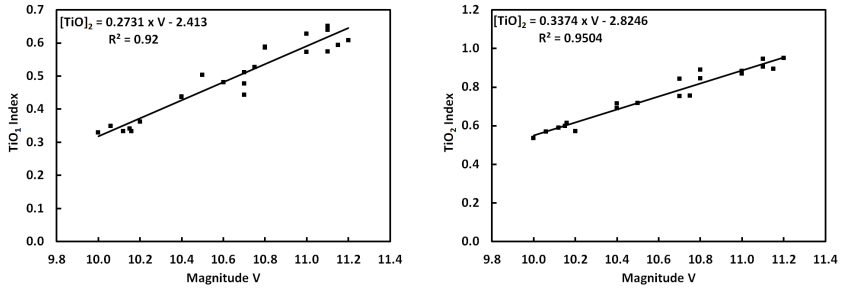

Figure 16a (left): TiO_1 index as a function of V magnitude. Figure 16b (right): TiO_2 index as a function of V magnitude.